JTTEE5 19:893–901
DOI: 10.1007/s11666-010-9514-z

Peer Reviewed

The Influence of Spraying Angle on Properties of HVOF Sprayed Hardmetal Coatings

Šárka Houdková, Michaela Kašparová, and František Zahálka

(Submitted September 3, 2009; in revised form April 26, 2010)

The spraying angle is one of the deposition parameters that influence the quality of thermally sprayed coatings. In theory, decreasing the spraying angle results in lower process deposition efficiency, whereas the porosity of coatings increases, becoming a cause of poorer microstructure and mechanical properties. In this study, the dependence of microstructure together with the basic mechanical properties and wear of WC-Co and Cr_3C_2-NiCr high-velocity oxyfuel (HVOF) sprayed coatings on the spraying angle was investigated. For each coating, the maximum spraying angle was determined that can be used without significantly decreasing coating quality. Based on the changes in properties of coatings and requirements for the process deposition efficiency, a maximum 30° diversion from the normal spray direction is recommended for WC-Co and 15° diversion for Cr_3C_2-NiCr coatings.

Keywords cermet, coating, Cr_3C_2-NiCr, HVOF, spraying angle, thermal spraying, WC-Co

1. Introduction

Tribological properties of surface, namely its wear resistance and friction properties, are in many cases decisive for the proper function of the part. In order to improve the surface properties, it is possible to create hard, wear-resistant coatings by thermal spray technologies. Optimum materials for creation of hard, wear- and corrosion-resistant coatings include ceramics and cermets. For spraying ceramics, which need to be melted at very high temperatures, the technology of choice is plasma spraying. For cermets, the best way is to use the high-velocity oxyfuel (HVOF) technology, which was developed for spraying cermets to produce high-quality coatings.

In HVOF thermal spraying, oxygen and fuel gas flow at high pressures and flow rates. Internal combustion takes place and results in very high particle velocities at relatively low temperatures compared with other thermal spray processes, such as air or vacuum plasma spraying (Ref 1). As a result, HVOF has the ability to produce dense coatings with a low degree of decomposition and with a good bond to the substrate. Because of the process parameters, the HVOF spraying process is the most suitable for spraying hard metals. As a line-of-sight process, HVOF is limited in application by the part geometry, particularly in coating surfaces in holes with small diameters (Ref 2). In practice, it is often impossible to use a 90° spraying angle. This can lead to significant changes in the coating properties. The off-angle impact of particles leads to the elongation of splats, the so-called shielding effect, resulting in an increase in porosity and surface roughness. The homogeneity of phase distribution in cermet coatings can also be negatively influenced by decreasing the spraying angle. The changes in coating microstructure are crucial for their properties, such as hardness, bond and cohesive strength, or wear resistance. The deposition efficiency, one of the most important economic parameters of the spraying process, is heavily dependent on the spraying angle. A high amount of sprayed material does not attach to the coating and is wasted.

In the literature, the influence of the spray angle has been studied in relation to microstructure, hardness, surface roughness, and deposition efficiency (Ref 2-6). The general opinion is that spraying at angles up to 45° guarantees a successful application with only a marginal loss of coating quality. To verify these statements for particular coating materials, an investigation into the spray angle influence on the deposition process and coating properties was conducted on HVOF TAFA JP-5000 sprayed WC-17%Co and Cr_3C_2-25%NiCr coatings. This study can provide a basis for determining the tolerance limits within which coatings exhibit reproducible properties.

2. Experimental Procedures

The coatings were sprayed using HP/HVOF JP-5000 (TAFA) spraying equipment at ŠKODA VÝZKUM s.r.o. in Pilsen onto grit-blasted carbon steel EN 10025-90 using the spray parameters that were previously optimized for a spray angle of 90° (Ref 7) to achieve the best microstructure, the highest hardness and microhardness, and

Šárka Houdková, Michaela Kašparová, and **František Zahálka**, ŠKODA VÝZKUM s.r.o, Tylova 1/57, Pilsen, Czech Republic. Contact e-mails: sarka.houdkova@skodavyzkum.cz, michaela.kasparova@skodavyzkum.cz, frantisek.zahalka@skodavyzkum.cz.

Table 1 Spraying conditions

Coating	Powder	Eq. ratio	Carrier gas	Barrel length, mm	Spraying distance, mm
WC-17%Co	FST K-674.23	0.8	Argon	150	380
Cr_3C_2-25%NiCr	TAFA 1375VM	0.8	Argon	150	360

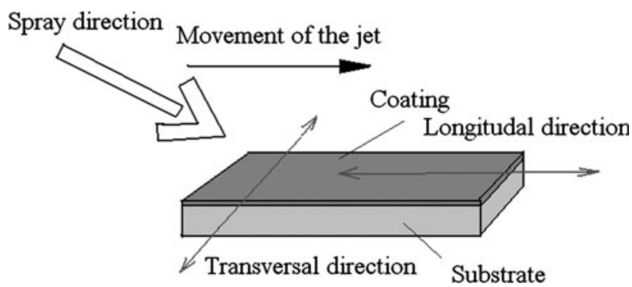

Fig. 1 Orientation of tested samples with respect to spraying direction

optimal deposition efficiency. Details of the spraying parameters are summarized in Table 1.

Five different spraying angles were used to spray the samples: 90°, 75°, 60°, 45°, and 30°. For each spraying angle, a different number of passes was applied to produce a similar coating thickness in all samples.

The coatings were then analyzed in terms of their microstructure, mechanical and physical properties, and deposition efficiency. Some properties, where possible and necessary, were analyzed in two perpendicular directions (longitudinal and transverse) with respect to the spraying direction, as shown in Fig. 1.

The microstructure of the coatings was evaluated using optical and scanning electron microscopy in two perpendicular directions. The homogeneity of hard particle distribution, the amount of pores, and the presence of cracks and other defects were analyzed. Microhardness was also measured in two perpendicular directions on the cross sections of the coatings using the Vickers indentation test at 300 g load and 10 s dwell time. At least 10 measurements were taken on each sample. The surface hardness was determined using the Rockwell HR15N method on the as-sprayed coating surface according to EN ISO 6508-1. At least five measurements were taken on each sample.

An estimate of the residual stress was obtained by the Almen strip test method based on a measurement of deflection of thin coated metal strips (Ref 8-10). The method is only suitable for qualitative assessment. For a quantitative analysis it would be necessary to use another method, for example, the incremental hole drilling method (Ref 11, 12).

The resistance of coatings to fracture propagation in brittle materials can be measured using the Vickers indentation method. The technique of indentation fracture toughness measurement, described in detail by Ponton (Ref 13), can be successfully used for the evaluation of thick brittle coatings (Ref 14-16). References 13 and 17 discuss 19 formulas for calculation of indentation fracture toughness. Their application to coatings results in different values of indentation fracture toughness, but their general rationale is the same (Ref 18). The values of indentation fracture toughness presented in this study were determined according to the Lawn and Swain formula (Ref 19) from the length of cracks propagating from the corners of the Vickers indentation made in the coating cross section at 200 N in WC-Co and 100 N in Cr_3C_2-NiCr. In each coating, at least seven indentations were made in two perpendicular directions.

$$K_{Ic} = 0.0101\left(\frac{L}{ac_{3/2}}\right) \quad \text{(Eq 1)}$$

where K_{Ic} is fracture toughness determined from the indentation tests, L is the indenter load, a is the half-length of the indentation diagonal, and c is the total crack length.

The coating density (g/cm^3) was determined according to Archimedes law from the weight of the sample measured in water and in air using Eq 2:

$$\rho = \frac{m_T \cdot \rho_V}{m_T - m} \quad \text{(Eq 2)}$$

where m_T is the coating weight in air (g), m is the coating weight in water (g), and ρ_V is the density of water (g/cm^3).

The deposition efficiency was evaluated according to EN ISO 17836 (Ref 20).

Wear resistance of the coatings was evaluated by the dry sand/rubber wheel test according to ASTM G-65 (Ref 21). The principle of the method makes it possible to evaluate three-body abrasive wear under low-stress conditions. Al_2O_3 with grain size of 212 to 250 μm was used as an abrasive medium. The rubber wheel was pressed against the coated sample with a load of 22 N along a sliding distance of 1.436 m. The wear is characterized by the wear rate, calculated from the coating volume loss and the sliding distance using Eq 3. At least three samples for each spraying angle were tested.

$$W_r = \frac{1000\, m_T/\rho}{s} \quad \text{(Eq 3)}$$

where m_T is the coating weight in air (g), ρ is the density of the coating (g/cm^3), and s is the sliding distance (m).

3. Results and Discussion

The main feature of off-angle spraying is a change in the ratio of the normal and tangential components of the spraying velocity. The normal component of the velocity is dominant down to 45°; below this limit the tangential component becomes dominant. The gradual mutation of dominancy from normal to tangential component influences the microstructure and consequently the properties of off-angle sprayed coatings.

At normal spray direction, the microstructure of the sprayed coating is formed by splats that are elongated parallel to the coating/surface boundary. During the first pass of the spray gun, the melted particles interlock on the rough substrate surface. Each further pass adds new splats, and the peening effect of impacting molten particles contributes to the compressive component of the inner coating stress. The properties of the coatings, such as porosity, hardness, cohesive strength, and so forth, depend on the kinetic energy of the impacting particles (provided the temperature of the particles is constant).

With decreasing spraying angle, the shape of the splats changes, as with the spraying direction. Up to 45°, the shielding effect, described in Ref 22 and confirmed by Tillmann (Ref 3), occurs and results in an increase in porosity and related decrease in density of the coating. The lower normal component of the spraying velocity weakens the peening effect, leading to reduced compressive stress. At low spraying angles, below the 45°, the influence of the tangential component of velocity starts to be important. While in the normal spray direction, all passes produced similar shapes of splats, low spraying angles result in a more complicated microstructure. The morphology of the splats created while the coated surface moves away from the spray gun differs from that of splats created while the coated surface moves toward the gun.

3.1 Microstructure of Coatings

The WC-17%Co powder for HVOF spraying consists of hard particles of WC, embedded in tough Co matrix. As a result of oxidation taking place during the deposition process, a part of the WC decomposes into W_2C and W, releasing CO and CO_2. Together with the oxidation process, dissolution of W and C in the Co matrix takes place. As a result of rapid solidification of droplets after impact, the matrix includes amorphous or fine-grained structures, which could later give rise to precipitation of W or so called η phases (in particular Co_3W_3C, Co_6W_6C). Decarburization and formation of brittle η phases are undesirable effects leading to the loss of the tough Co matrix. The presence of the aforementioned phases in HVOF sprayed WC-Co coatings was described in the literature many times (Ref 23, 24).

Microstructure of the Cr_3C_2-25%NiCr coating also includes, besides hard Cr_3C_2 carbides and the NiCr matrix, Cr_2O_3. It is formed by the oxidation process during spraying. The microstructure also includes lower Cr_7C_3 and $Cr_{26}C_6$ carbides with hardness lower than that of the initial Cr_3C_2, produced by a decarburization process similarly to the WC-Co. Because of dissolution of carbides in the matrix, the concentrations of C and Cr in the matrix of the coating are higher when compared with the powder material. It enables the melted droplets to solidify as a quasi-amorphous or nanocrystalline structure. Other nanocrystalline phases, with a grain size around 10 nm, formed of Ni and Co appear in the coating microstructure as a result of rapid solidification (Ref 24, 25).

The microstructure of all studied WC-Co coatings (Fig. 2a-e) is homogeneous, without cracks or unmelted particles. Only a minor amount of pores is present in the coating, and the carbide distribution in the matrix is uniform. In the case of the Cr_3C_2-NiCr coating (Fig. 3a-e), the microstructure shows no visible changes up to the spray angle of 75°. Coatings sprayed at 60° and lower angles showed longitudinal and lateral cracks (Fig. 4), which were also present along the substrate/coating boundary. This indicates that there was a high tensile stress in the coating. The effect of the spraying angle on the microstructure is visible in the changed shape of splats. By contrast, only negligible changes in porosity were observed in both coatings, despite the expected effect of shielding (Ref 22) and results of the Tillmann (Ref 3) study, which focused on APS WC-Co and Cr_3C_2-NiCr coatings. Moreover, the amount of porosity in coatings sprayed at 30° is lower than in the coatings sprayed at 60° and 45°. The study by Strock et al. (Ref 2), concerning the HVOF sprayed WC-CoCr coatings confirmed the observation that the distribution of phases is more uniform across the surface in the off-angle coatings.

The microstructure of the evaluated cermet coatings consists of hard particles (WC in WC-Co coatings, Cr_3C_2 in Cr_3C_2-NiCr coatings), embedded in a tough matrix. Because of the processes taking place during deposition, such as oxidation, decarburization, or rapid solidification, some other phases, such as lower carbides, brittle η phases or oxides appear in the coatings. Their presence is well known and has been described in literature many times (Ref 23-25). None of the studied WC-Co coatings (Fig. 2a-e) contains any cracks or unmelted particles; they typically exhibit only low porosity. The Cr_3C_2-NiCr coating (Fig. 3a-e) sprayed at 60°, and lower angles showed longitudinal and lateral cracks (Fig. 5), also present along the substrate-coating boundary, indicating high tensile stress in the coating.

Off-angled spraying influenced the shape of the splats and their orientation, but not the amount of porosity, despite the expected effect of shielding (Ref 22) and results of the Tillmann (Ref 3) study, which focused on APS WC-Co and Cr_3C_2-NiCr coatings. This contradiction can be explained by high spraying velocity leading to a higher elongation and flattening of the splats at low angles, which leads to better splat blending and also lower roughness values (Fig. 9). The same effect was observed by Strock et al. (Ref 2) in HVOF sprayed WC-CoCr coatings.

Particular attention should be paid to coatings sprayed at 30°. In the microstructure of the coatings (Fig. 5) parallel areas corresponding to individual passes can be recognized. Uniformly distributed carbides and low porosity characterize those passes when the coated surface moved away from the spray gun. The splats created during this pass are sloping in direction, perpendicular to the direction of spraying. The next pass, when the coated surface

Peer Reviewed

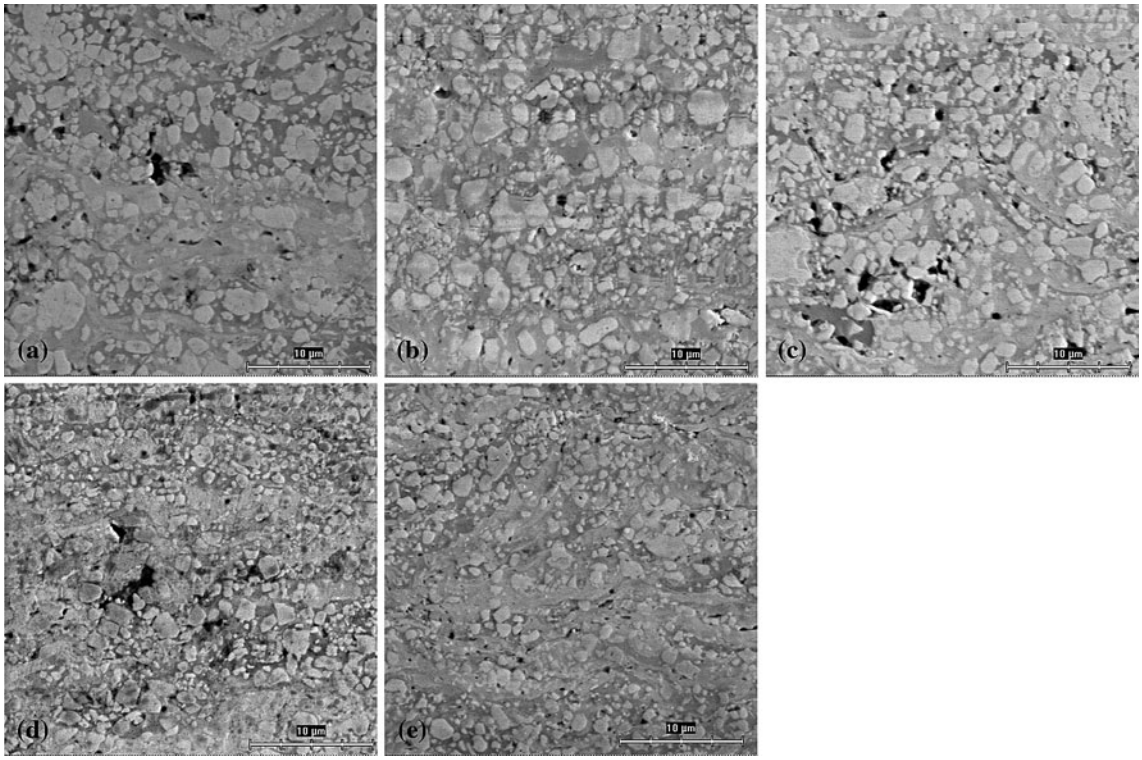

Fig. 2 Microstructure of WC-Co coatings, sprayed at different angles: (a) 90°, (b) 75°, (c) 60°, (d) 45°, and (e) 30°

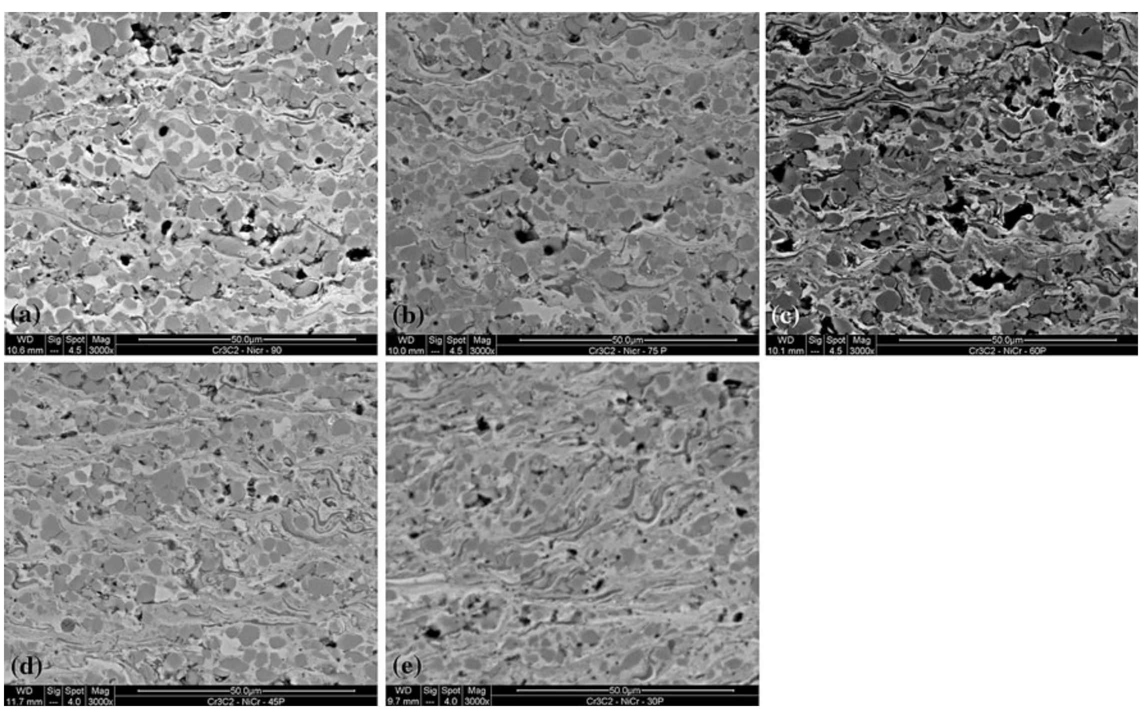

Fig. 3 Microstructure of Cr_3C_2-NiCr coatings, sprayed at different angles: (a) 90°, (b) 75°, (c) 60°, (d) 45°, and (e) 30°

moves toward the spray gun, is characterized by a low amount of carbides. The growth of the coating during this pass is much slower and the shape of the splats cannot be identified. The rebounding of carbides, similar to the effect described in Ref 26 during this pass, is responsible for the loss of carbides (Fig. 2e, 3e, and 4).

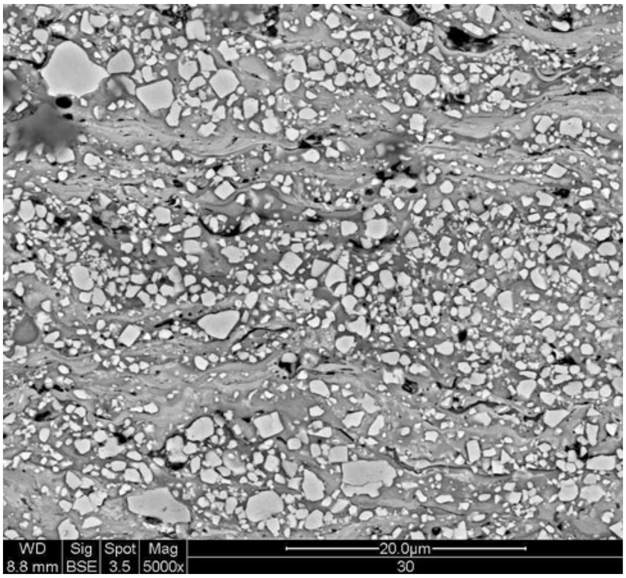

Fig. 4 Microstructure of WC-Co coating, sprayed at 30°

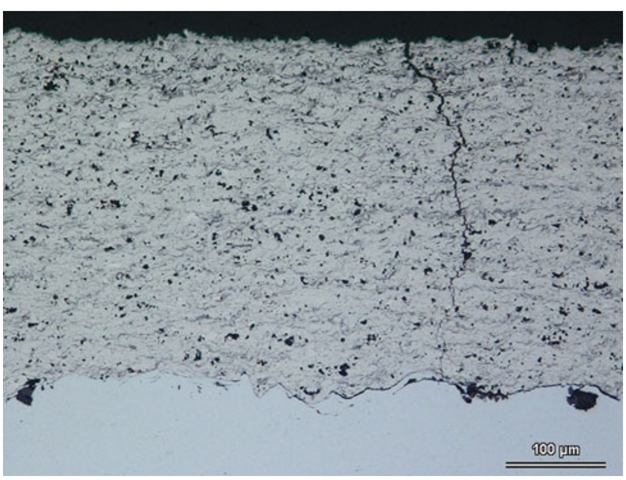

Fig. 5 Cracks in the off-angle Cr_3C_2-NiCr coating

The significant effect of two alternating layers in the coating was observed only for coatings sprayed at 30°, when the tangential component of the spraying velocity is dominant. With the changed microstructure, changes in the related properties appeared.

3.2 Hardness and Microhardness

As expected, the hardness and microhardness of the WC-Co coating were higher when compared with the Cr_3C_2-NiCr coating. The surface hardness of both coatings showed a decrease in values for the 75° spray angle, followed by an unexpected increase for the 60° spray angle. Beyond that the HR15N values decreased with the spray angle. With respect to the measurement scatter, no significant dependence of surface hardness on the spraying angle was found. The surface hardness measurement, due

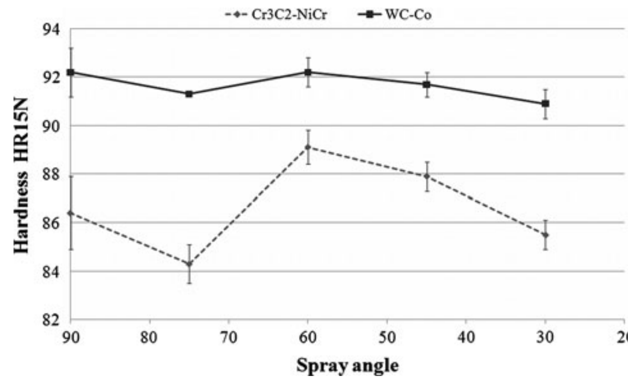

Fig. 6 Superfacial hardness in dependence on spraying angle

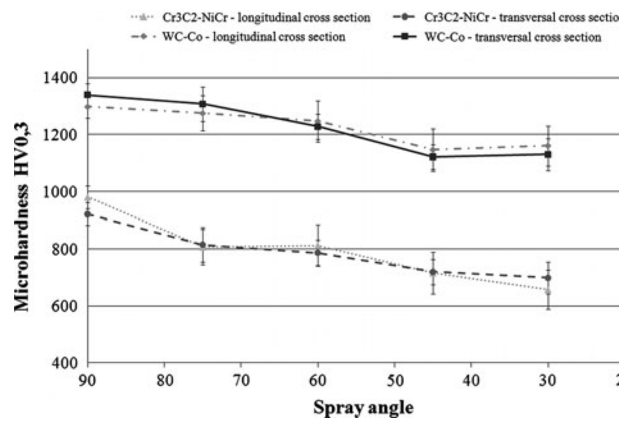

Fig. 7 Microhardness in dependence on spraying angle

to a high load, involves information from a big volume of coating material, including the pores and splat boundaries. The negligible changes of the off-angle coating microstructure do not evoke the significant changes of surface hardness.

On the contrary, the microhardness, measured at 300 g, involves the information only from a few splats. The hardness of single phases plays a bigger role as well as the bond strength of hard phases to the matrix and the bond strength between splats.

The microhardness values showed a continuous decrease with the decreasing spray angle, which is in correlation with the results by Strock et al. (Ref 2). The hardness and microhardness results are shown in Fig. 5 and 6.

As expected, the hardness and microhardness of the WC-Co coating were higher when compared to the Cr_3C_2-NiCr coating (Fig. 7). With respect to the measurement scatter, no significant dependence of surface hardness on the spraying angle was found. Conversely, the microhardness values showed a continuous decrease with decreasing spray angle, which correlates with the results from Strock et al. (Ref 2). The surface hardness measurement, due to the high load, collects information from a large volume of the coating material, including the pores and splat boundaries. The negligible changes in the off-angle coating microstructure do not result in any significant changes in the surface hardness. The microhardness, measured at 300 g, provides information on only a few splats. The hardness of single phases plays a greater role as well as the bond strength of hard phases to the matrix and the bond strength between splats.

3.3 Residual Stress

Generally speaking, HVOF coatings tend to have a compressive residual stress as a result of the high-impact velocities of droplets, which is beneficial for their properties. The peening effect of impacting particles is highest when the normal spray direction is used. With decreasing spraying angle the normal component of the impact velocity decreases and the shrinkage tensile stress, naturally present in the coating as a result of solidification, becomes dominant (Ref 27). In our case, compressive residual stress was found in the WC-Co coating only, while tensile residual stress was present in the Cr_3C_2-NiCr coating. The tensile stress component increased with the spray angle decreasing below 90° in both coatings, in agreement with Strock et al. (Ref 2). At 30° spray angle, the level of tensile stress decreased in both coatings (Fig. 8). When the surface being coated moves away from the spray gun during low-angle spraying, a peening effect of impacting particles in the spraying direction in one pass occurs as a result of the tangential component of the spraying velocity.

Although at 30° spray angle, the level of tensile stress slightly decreased (Fig. 7), increasing tensile stress level with decreasing spray angle has also been observed by Strock et al. (Ref 2).

3.4 Indentation Fracture Toughness

The resistance of the WC-Co coating to fracture propagation expressed as K_{Ic} decreased as the spray angle decreased below 90°, with a slight increase at 60° (Fig. 9). The tendency is similar to the behavior of surface hardness HR15N (see Fig. 6). The Cr_3C_2-NiCr appeared more brittle than the WC-Co coating. The cracks were considerably longer, and the scatter of results was much higher. The dependence on spray angle was not as significant as in the WC-Co coating. No significant dependence of K_{Ic} on the spray angle was observed. Either the spray angle does not influence the Cr_3C_2-NiCr cracking behavior, or, more probably, the dependence is below the resolution limit of the method used. The same effect as in the case of residual stress is responsible for lower intersplat cohesion of the coating. The cohesion of the splats also depends on the normal component of the impact energy, which decreases with decreasing spraying angle.

3.5 Surface Roughness

In both coatings, the surface roughness expressed by R_a decreased with the spray angle decreasing below 90° with the exception of 30° sprayed WC-Co coatings, where a slight increase was noted (Fig. 10). In both cases,

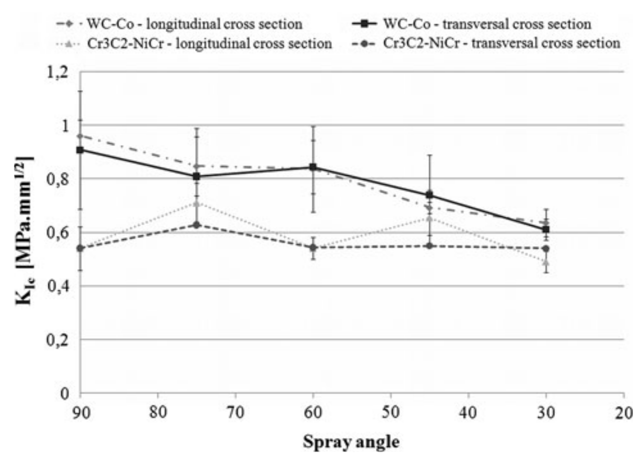

Fig. 9 Indentation fracture toughness in dependence on spraying angle

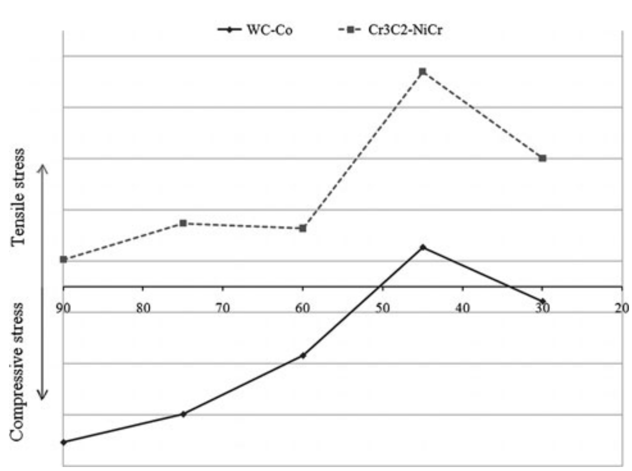

Fig. 8 Residual stress in dependence on spraying angle

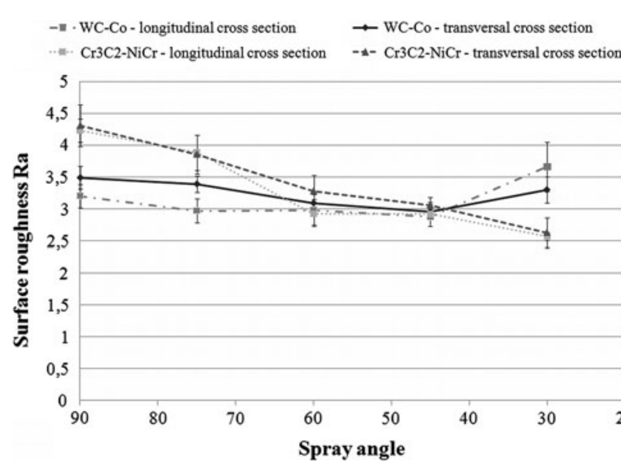

Fig. 10 Surface roughness in dependence on spraying angle

the surface roughness in the longitudinal direction is slightly higher when compared with the R_a value measured in the transverse direction. A decrease in R_a together with the spraying angle was also observed by Strock et al. (Ref 2) and Bach et al. (Ref 6). The more elongated shape of splats in the case of HVOF off-angle spraying (Ref 2) as well as the possible abrasive effect of off-angle impinging particles is mentioned (Ref 6). Both can play a role in decreasing the surface roughness of off-angle sprayed coatings. Tillmann et al. (Ref 3) presents an opposite tendency of APS sprayed coatings at a spray angle lower than 50°. APS spraying uses lower spraying velocities, where the energy for the abrasive action is not as large. Instead, the probability of sprayed particles at low spraying angles to interlock with surface asperities inhomogeneities is higher. Nevertheless, the observed decline in R_a is a positive finding from the technological viewpoint: It means that there is no need to increase the machining allowance in case the of off-angle sprayed coatings.

3.6 Specific Density

Specific density of the coatings was measured by a method based on Archimedes law. The differences in values of specific density represent the different levels of porosity in the coatings. The results are shown in Fig. 11. The WC-Co density, and to a lesser degree also the Cr_3C_2-NiCr density, confirm the theory of the importance of the ratio of the normal/tangential component of spraying energy. The density of the coatings, with respect to the measurement error, decreases with declining spraying angle down to 45°. For lower spraying angle, a sudden increase in density, correlating with the result of the microstructure evaluation, can be observed. The density measurement, with respect to the measurement error, does not exhibit any clear dependence on the spray angle. A sudden increase in density of coatings sprayed at 30°, correlating with the result of the microstructure evaluation, can be observed.

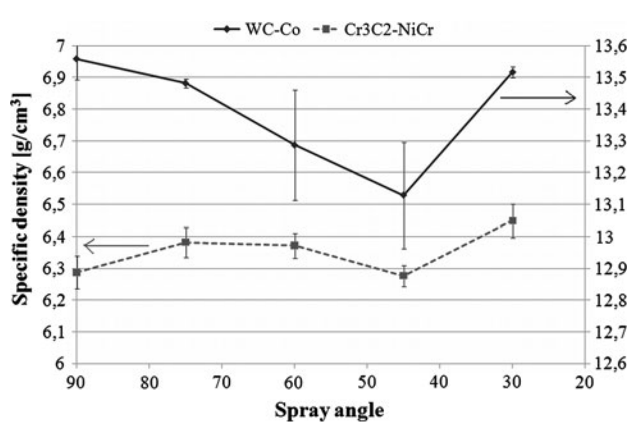

Fig. 11 Specific density in dependence on spraying angle

3.7 Deposition Efficiency

The results obtained (Fig. 12) clearly show that the deposition efficiency strongly depends on the spray angle. The same was confirmed by results presented by Tillmann et al. (Ref 3). During off-angle spraying, a certain part of the sprayed particles does not attach to the surface. The normal component of the spraying velocity is the main factor responsible for the deposition efficiency (Ref 27). In the case of low spraying angle, the growth of the coating in the pass, when the coated surface moves toward the spray gun, is strongly limited.

Moreover, the abrasive effect of off-angle impinging particles also decreases the amount of deposited material. The deposition efficiency is one of the main parameters that affect the economy of the thermal spray process. From this viewpoint, it is noticeable that the process of spraying is not very effective even at a 90° spray angle (only 40% deposition efficiency).

3.8 Wear

The abrasive wear rate of the coatings in dependence on the spraying angle is represented in Fig. 13. The wear resistance of the WC-Co coating is approximately five

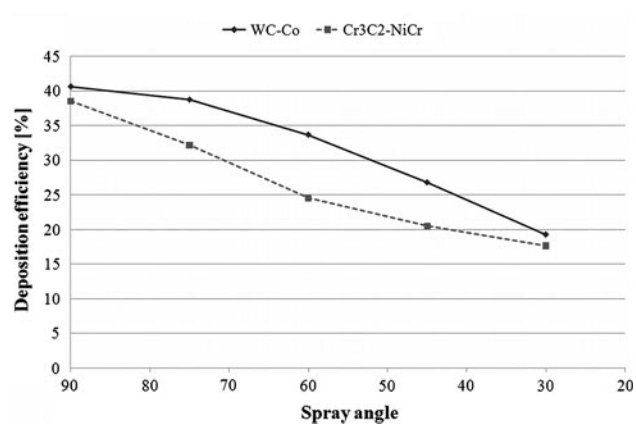

Fig. 12 Deposition efficiency in dependence on spraying angle

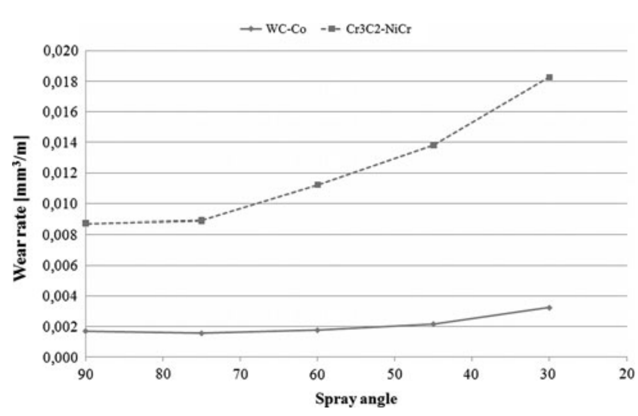

Fig. 13 Wear rate in dependence on spraying angle

Peer Reviewed

times higher compared with the Cr_3C_2-NiCr coating. Both coatings met the expectation of declining wear resistance with a decrease in the spraying angle. For the WC-Co coating, the difference between the wear rate of coatings sprayed at 90°, 75°, and 60° was very small, and the wear resistance in these cases can be considered equal. The coatings sprayed at lower spray angles, especially at 30°, showed significantly poorer wear behavior. In Cr_3C_2-NiCr coatings, equivalent wear behavior can be observed in coatings sprayed at 90° and 75°.

The mechanism of wear was studied using scanning electron microscopy (SEM). The micrographs of the worn surface correspond with the wear rate values. The wear mechanism of a coating sprayed perpendicularly to the surface can be characterized by a gradual loss of the metal matrix followed by a drop-in carbide/matrix cohesion and pulling off carbides. Coatings sprayed at lower angles exhibit massive wear damage represented not only by pulling off carbides, but also by pulling off parts of the splats themselves. Such behavior indicates a low intersplat cohesion in the off-angle coating. The low intersplat cohesion is also connected with the results of indentation fracture toughness. The abrasive wear resistance of materials depends on basic mechanical properties—microhardness and toughness. Both decrease with the spraying angle. There are several theoretical models predicting that the wear rate depends on the hardness and toughness of thermally sprayed coatings (Ref 28, 29), but the results of measured wear rate in our experiment are not in agreement with the wear rate predicted by these models. In the theoretical models, an attempt to take into consideration the coating microstructure using constants was made, but the wear process of thermally sprayed cermet coatings is still too complex to be expressed by a simple equation. The results of the dry sand/rubber wheel test are in contradiction to the results by Strock et al. (Ref 2), who found an opposite dependence in the fretting wear test. In spite of their lower hardness and lower compressive residual stress, the off-angle WC-CoCr coatings exhibited less wear damage than the 90° coatings. He explained this unexpected behavior by the more uniform distribution of phases across the surface in the off-angle coatings, which was not observed in our case. The contradiction could also be caused by differences between wear conditions of the fretting and the abrasive wear test.

4. Conclusions

The evaluation of the influence of the spray angle on physical, mechanical, and technological parameters of HVOF hard metal coatings showed that coating properties are variously sensitive to the spray angle. While the coating microstructure, microhardness, residual stress, wear rate, and deposition efficiency showed strong dependence on the spray angle, the dependence of density, surface hardness, indentation fracture toughness, and the surface roughness on spray angle is rather weak; only some of their properties depend on the spray angle. Analysis of the results revealed some interesting correlations. The trends of the behavior of surface hardness and indentation fracture toughness of the WC-Co coating are similar. Results of microhardness and residual stress measurements correspond to each other, but not to surface hardness and indentation fracture toughness, although such similarity could be expected. The explanation could involve the load range used for the measurement. Microhardness values measured at a load of 300 g were obtained from an area of several splats, while the surface hardness measured at a load of 15 kg comprises information from a greater volume of the coating—as does the indentation fracture toughness (20 kg). The surface hardness and the indentation fracture toughness measurements took place on the same microstructure ''scale'' and are influenced by the coating microstructural features: pores, oxides, splat boundaries, and so forth, while the microhardness measurement is closer to the measurement of a bulk material.

The surprising properties of the coatings sprayed at 30°, namely the density, microhardness, residual stress, and surface roughness being better than in coatings sprayed at 45°, are connected with the changes in the coating microstructure. The morphology of splats differs in the case of low-angle spraying, when the tangential component starts to become important. The two mechanisms of splat assembling take effect during different passes—the effective one, when the coated surface moves away from the spray gun, and the ineffective one, when the coated surface moves towards the gun. The first is characterized by a low number of pores, uniformly distributed carbides, higher peening effect, and faster growth of the coating, whereas the second exhibits loss of carbides by the rebounding effect (Ref 26) and very slow coating growth. The altered microstructure leads to unexpected changes in related properties of the coatings that could be affected by the peening effect. The properties of the WC-Co coatings sprayed at 30° are surprising in general. Contrary to the expectation, their microstructure, density, microhardness, residual stress, and surface roughness are better when compared with the coatings sprayed at 45°. In case of the Cr_3C_2-NiCr coating, the same effect was only observed in relation to density and the residual stress. The process of carbides rebounding during HVOF spraying described in Ref 26 can be responsible for changes in coating microstructure and related properties, but the mechanism of carbide rebounding of off-angle sprayed coatings was not sufficiently explained. However, regardless of the mechanical and physical properties of the coatings sprayed at 30°, no increase in their wear resistance was observed. This is probably caused by low intersplat cohesion related to a low normal component of spraying velocity, imperfect spreading, and the placement of droplets on the forming coating during low-angle spraying. Based on the measured data, the use of a spray angle of up to 60° for the WC-Co HVOF coating, and up to 75° for the Cr_3C_2-NiCr HVOF coating can be recommended. These coatings are fully acceptable both from the functional and the economical viewpoints.

Acknowledgment

This paper was prepared thanks to project of the Czech Ministry of Education No. MSM 4771868401.

References

1. E.B. Smith, T.J. Power, and T.J. Barber, United Technology Research Centre Report, East Hartford, CT, 1991, p 91
2. E. Strock, P. Ruggiero, and D. Reynolds, The Effect of Off-Angle Spraying on the Structure and Properties of HVOF WC/CoCr Coatings, *Thermal Spray 2001: New Surfaces for a New Millennium,* C.C. Berndt, K.A. Khor, and E.F. Lugscheider, Ed., May 28-30, 2001 (Singapore), ASM International, 2001, p 671-676
3. W. Tillmann, E. Vogli, and B. Krebs, Influence of the Spray Angle on the Characteristics of Atmospheric Plasma Sprayed Hard Material Based Coatings, *J. Therm. Spray Technol.*, 2008, **17,** p 948-955; also in *Thermal Spray 2008: Crossing Borders*, B.R. Marple, M.M. Hyland, Z.-C. Lau, C.-J. Li, R.S. Lima, and G. Montavon, Ed., June 2-4, 2008 (Maastricht, NL), ASM International, 2008, p 235-240
4. M.F. Smith, R.A. Neiser, and R.C. Dykhuizen, An Investigation of the Effects of Droplet Impact Angle in Thermal Spray Deposition, *Thermal Spray Industrial Applications*, C.C. Berndt and S. Sampath, Ed., June 20-24, 1994 (Boston, MA), ASM International, 1994, p 603-608
5. S.H. Leigh and C.C. Berndt, Evaluation of Off-Angle Thermal Spray, *Surf. Coat. Technol.*, 1997, **89**, p 213-224
6. Fr.-W. Bach, K. Möhwald, and L. Engl, Roughness Enhancement of HVOF Sprayed MCrAlY Bond Coatings for Adhesion Improvement of Ceramic Top Layers, *Thermal Spray 2006: Science, Innovation, and Application*, B.R. Marple and C. Moreau, Ed., May 15-18, 2006, ASM International, 2006, p 649-654
7. Š. Houdková, R. Enžl, P. Fiala, and O. Bláhová, Mechanical Properties of HVOF Coatings, *Proceedings of University of West Bohemia*, 2001, University of West Bohemia, 2002, p 73-83
8. J.J. Han and R. Knight, Residual Stresses in HVOF-Sprayed Cr_3C_2/NiCr Coatings, *Tagungsband Conference Proceedings*, E. Lugscheider and R.A. Kammer, Ed., March 17-19, 1999 (Düsseldorf, Germany), DVS Deutscher Verband für Schweiβen, 1999, p 771-776
9. "Test Strip, Holder, and Gage for Shot Peening," SAE J442, Revised Dec 2001
10. "Procedures for Using Standard Shot Peening Test Strip," SAE J443, Revised Jan. 2003
11. M. Ecribano, R. Gadow, and M. Buchmann, Residual Stress Analysis in Thermally Sprayed Layer Composites, Using the Microhole Milling and Drilling Method, *Thermal Spray 2003: Advancing the Science and Applying the Technology*, B.R. Marple and C. Moreau, Ed., May 5-8, 2003 (Orlando, FL), ASM International, 2003, p 1297-1305
12. Y.Y. Santana, P.O. Renault, M. Sebastiany, J.G. La Barbera, J. Lasage, E. Bemporad, E. Le Bourhis, E.S. Puchi-Cabrera, and M.H. Staia, Characterisation and Residual Stress of WC-Co Thermally Sprayed Coatings, *Surf. Coat. Technol.*, 2008, **18**(202), p 4560-4565
13. C.B. Ponton and R.D. Rawlings, Vickers Indentation Fracture Toughness Test Parts 1 and 2, *Mater. Sci. Technol.*, 1989, **5**, p 865-872
14. H. Li, K.A. Khor, and P. Cheang, Young's Modulus and Fracture Toughness Determination of High Velocity Oxy-Fuel-Sprayed Bioceramic Coatings, *Surf. Coat. Technol.*, 2002, **155**, p 21-32
15. H.P. Brantnrer, R. Pippan, and W. Prantl, Local and Global Fracture Toughness of Flame Sprayed Molybdenum Coatings, *J. Therm. Spray Technol.*, 2003, **12**, p 560-571
16. C. Giolli, A. Scrivani, G. Rizzi, F. Borgioli, G. Bolelli, and L. Lusvarghi, Failure Mechanism for Thermal Barrier Coating Systems, *Thermal Spray 2008: Crossing Borders*, B.R. Marple, M.M. Hyland, Z.-C. Lau, C.-J. Li, R.S. Lima, and G. Montavon, Ed., June 2-4, 2008 (Maastricht, Netherlands), ASM International, 2008, p 460-467
17. C.B. Ponton and R.D. Rawlings, Vickers Indentation Fracture Toughness Test. Part 2, *Mater. Sci. Technol.*, 1989, **5**, p 961-976
18. Š. Houdková, R. Enžl, F. Zahálka, and O. Bláhova, The Indentation Tests for Evaluation of HVOF Coatings' Mechanical Properties, *Thermal Spray Connects: Explore its Surfacing Potential*! E. Lugscheider, Ed., May 2-4, 2005 (Basil, Switzerland), DVS Deutscher Verband für Schweiβen, 2005, p 1521-1525
19. B.R. Lawn and M.V. Swain, Microfracture Beneath Point Indentation in Brittle Solids, *J. Mater. Sci.*, 1975, **10**, p 113-122
20. "Thermal Spraying—Determination of the Deposition Efficiency for Thermal Spraying," EN ISO 17836, International Organization for Standardization, 2004
21. "Standard Test Method for Measuring Abrasion Using the Dry Sand/Rubber Wheel Apparatus," G 65, ASTM International, West Conshohocken, PA, 2001
22. J.R. Davis, *Handbook of Thermal Spray Technology*, ASM International, Materials Park, Ohio, 2004
23. R. Schwetzke and H. Kreye, Microstructure and Properties of Tungsten Carbide Coatings Sprayed with Various High Velocity Oxygen Fuel Spray System, *J. Therm. Spray Technol.*, 1999, **8**, p 433-439
24. L.-M. Berger, Chemistry of Carbide-Metal Composites for Preparation of HVOF Sprayed Coatings, Papers, Materials Week 2001, *Int. Conf. on Adv. Mater., their Processes and Applications,* Oct 1-4, 2001 (München, Germany), p 10
25. S. Zimmermann and H. Kreye, Chromium Carbide Coatings Produced with Various HVOF Spray Systems, *Thermal Spray: Practical Solutions for Engineering Problems*, C.C. Berndt, Ed., Oct 7-11, 1996 (Cincinnati, OH), ASM International, 1996, p 147-152
26. C.H.-J. Li, G.-Ch. Ji, Y.-Y. Wang, and K. Sonoya, Dominant Effect of Carbide Rebounding on the Carbon Loss During High Velocity Oxy-fuel Spraying of Cr_3C_2-NiCr, *Thin Solid Films*, 2002, **419**, p 137-143
27. C.-J. Li, W.-Y. Li, Y.-Y. Wang, and H. Fukanuma, Effect of Spray Angle on Deposition Characteristics in Cold Spraying, *Thermal Spray 2003: Advancing the Science and Applying the Technology*, B.R. Marple and C. Moreau, Ed., May 5-8, 2003 (Orlando, FL), ASM International, 2003, p 91-96
28. L.C. Erickson, H.M. Hawthorne, and T. Troczynski, Correlations Between Micro-Structural Parameters, Micromechanical Properties and Wear Resistance of Plasma Sprayed Ceramic Coatings, *Wear*, 2001, **250**, p 569-575
29. G. Bolelli, V. Cannillo, L. Lusvarghi, and S. Ricco, Mechanical and Tribological Properties of Electrolytic Hard Chrome and HVOF-Sprayed Coatings, *Surf. Coat. Technol.*, 2006, **200**, p 2995-3009